Current status and future perspectives of EU ceramic breeder development

Oliver Leys *, Julia M. Leys, Regina Knitter

Institute for Applied Materials (IAM), Karlsruhe Institute of Technology (KIT), Karlsruhe, Germany

ABSTRACT

Biphasic ceramic pebbles, consisting of Li_4SiO_4 and Li_2TiO_3, are being developed as the EU reference tritium breeding material for ITER and DEMO. A modified melt-based process for the pebble fabrication was established and optimised with regard to the process stability and yield. In parallel, the properties of pebbles and pebble beds were evaluated in dedicated experiments. These include investigations into e.g. the long-term thermal stability of pebbles, the thermomechanical properties of pebble beds, as well as the compatibility between the ceramics and the structural material. The available data was recently summarised and issued as the Material Property Handbook on Advanced Ceramic Breeders. During the EU DEMO conceptual phase, two main issues are proposed to be pursued in view of ITER. Irradiation campaigns are planned to ensure that the advanced ceramic breeder material is adequately tested and an extensive process scale-up with an increased production rate is foreseen to secure the supply for the ITER test blanket modules.

1. Introduction

The aim of the ceramic breeder (CB) material development during the pre-conceptual design phase of the EU DEMO was to strengthen the technical basis and to resolve the main technical issues associated with the tritium breeding ceramics for the solid breeder blanket concept. The activities were focused on developing and qualifying the breeding ceramics and their production process to an appropriate level to support the conceptual design review of the helium cooled pebble bed (HCPB) concept.

In the past, CB pebbles consisting of lithium orthosilicate and lithium metasilicate and produced by a melt-spraying technique were considered as the EU candidate for the HCBP blanket [1]. This material was extensively studied; however, concerns were raised especially regarding their mechanical behaviour.

For this reason, so-called advanced ceramic breeder (ACB) pebbles that also contain lithium metatitanate (Li_2TiO_3, abbr. 'LMT') besides lithium orthosilicate (Li_4SiO_4, abbr. 'LOS') were investigated for the first time with the aim of enhancing the mechanical properties [2]. In parallel, a new, modified melt-based fabrication process for the production of CB pebbles was developed with the intent of offering a better process control compared to the formerly used melt-spraying technique [3].

The primary objectives in the pre-conceptual phase were to establish a well-controlled fabrication process and to build up a reliable database of the material properties. Key aspects of the work performed were the optimisation of the production process, the selection of the optimum composition of the breeder pebbles and the determination of design relevant properties of advanced, mixed-phase breeder pebbles and pebble beds (PB). Details of the material and PB properties were recently summarised in a Material Property Handbook on ACB [4]. In the following, the state of the process and material development of EU ACB are summarised and an outlook on future activities is given.

2. Process development

Presently, a lab-scale facility, KALOS (KArlsruhe Lithium OrthoSilicate), is available for the melt-based production of ACB pebbles. The pebbles are produced in a batch process where the batch size is limited to about 1 kg due to the volume of the melting crucible. Taking into account the time to heat up and cool down the facility, only one batch can be produced per day, while the actual time to process 1 kg takes approximately 30 minutes.

The raw materials, lithium hydroxide monohydrate ($LiOH·H_2O$), silicon dioxide (SiO_2) and titanium dioxide (TiO_2), are mixed and thermally pre-treated to remove water and are then filled into a platinum alloy melting crucible (Fig. 1, left). After reaching a temperature of 1300–1400 °C (depending on the composition), a jet is generated by applying a pressure to the system and ejecting the melt through a small nozzle. Droplets are subsequently formed by the break-up of the jet and are solidified using a liquid nitrogen spray. The produced pebbles are
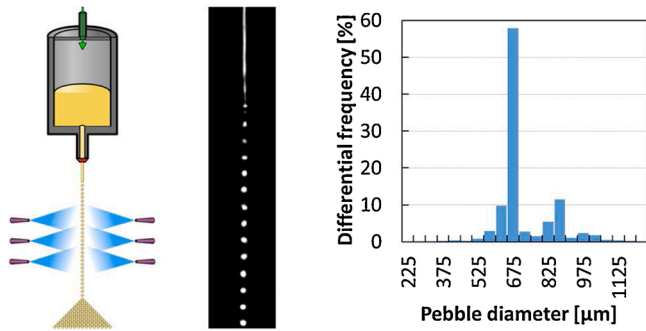

Fig. 1. Schematic of the KALOS process (left), video image of the droplet generation (middle), pebble size distribution (right).

screened to a diameter range of 250–1250 μm with a process yield of ≥90 wt.%.

The size of the generated droplets, and thus the resulting size of the pebbles, is determined predominantly by the diameter of the used nozzle, meaning it can be adjusted by employing a different nozzle. With the presently used nozzle diameter of 300 μm, a pebble size of approx. 650 μm is generated. The facility exhibits an elaborate process control; e. g. the monitoring of the droplet generation using a high-speed camera (Fig. 1, middle). The influence of the process pressure on the droplet generation, the size of the droplets and their velocity as a function of the nozzle size was extensively investigated to increase the process stability and yield [5,6].

To improve the process stability and yield, an induced jet break-up technique has recently been implemented into the process [7]. This also increased the monodispersity of the droplets, yet it should be noted that the aim is not to produce monosized pebbles. In principle, the pebbles are formed from single droplets, yet due to the coalesence of some droplets, a certain amount of pebbles with a double or triple volume are also formed (Fig. 1, right).

As a melt-based process in principle offers the advantage of a simple reprocessing of CB pebbles [8], the remelting and simulated re-enrichment of lithium was studied with regard to the accumulation of impurities and the perpetuation of properties [9]. It was demonstrated that the only impurities accumulated by remelting (Pt, Rh and Au) are caused by a slight corrosion of the Pt alloy crucible and that the properties of the pebbles are maintained after multiple remelting cycles as well as after reprocessing by re-enrichment. This also means that the amount of impurities, including those that are critical with regard to activation such as Co, only depends on the purity of the selected raw materials.

The production capacity of the present KALOS facility is limited by the batch size of 1 kg. Considering the time and effort for the production as well as for the characterisation, it is presently impossible to provide a larger quantity in an economic, efficient and effective way and in a timely manner. A medium sized production capacity should be realised in view of the planned testing of breeder blanket mock-ups as well as for the ITER test blanket modules (TBM). It was therefore decided to build a scale-up of the KALOS facility, preferably with a transition to a continuously operated process with a target production rate of 5–10 kg/d. Considering the current (theoretical) production rate of about 2 kg/h, this target appears to be feasible and readily attainable. It is planned that the upgraded KALOS facility is ready for operation in 2023. Especially with regard to the approx. 100 kg for the ITER TBM, it is necessary to define a quality control procedure to ensure that the produced pebbles fulfil the specification. The aim is to minimise the effort for characterisation while maintaining the reliability of the results.

Recently a roadmap has been developed to secure the future delivery and self-sufficiency of CB pebbles for the ITER TBM. In this roadmap, a cost estimate for the process scale-up, the procurement of Li-6 enriched raw materials and the fabrication of 100 kg of ACB pebbles, as well as a

time schedule and a possible procedure for the fabrication and characterisation of the pebbles, are given together with a brief risk evaluation. It was estimated that an enrichment of 90 % Li-6 will increase the total procurement costs by a factor of 3.5 to 4. While 80 % of the total procurement costs will account for the Li-6 enriched raw materials, in the case of natural (non-enriched) ACB pebbles, the total costs depend strongly on the chosen purity of the raw materials and will account for between 26 % for standard and 49 % for high purity synthesis powders.

3. Material development and evaluation

The combination of LOS and LMT was chosen for the ACB pebbles with the aim to combine the advantageous properties of both CB candidates, i.e. maintaining the high Li density of LOS as far as possible, while improving the mechanical properties with additions of LMT. Yet, because the Li-rich region of the ternary phase diagram Li_2O-SiO_2-TiO_2 had hardly been investigated in the past, no information on phase stability, solubility or melting temperatures was available in literature.

3.1. Fundamental properties of ACB pebbles

The basic properties of LOS pebbles with additions of 5–40 mol% LMT were investigated. Higher LMT contents were excluded, on the one hand because of the decreasing Li density (cf. Fig. 2) and on the other hand because of the increasing melting temperature that cannot be realised in the KALOS facility.

It was found (i) that no solubility exists in this region between the two phases, and (ii) that there is a eutectic at about 80/20 mol% LOS/ LMT with a melting temperature of approx. 1200 °C. During fabrication and due to the rapid cooling, the LMT phase solidifies in the cubic high-temperature phase, γ-Li_2TiO_3, but this phase is rapidly transformed to the stable, monoclinic β-Li_2TiO_3 by heat treatment (Fig. 3). A significant increase in the mechanical strength is only observed beyond the eutectic, i.e. at LMT contents of > 20 mol% LMT (Fig. 4).

After evaluating all investigated properties and the processability of the mixtures, a composition of 65/35 mol% LOS/LMT was defined as the optimum target composition for DEMO. However, this composition may be subject to change, because the behaviour under neutron irradiation has not yet been investigated.

Because of the melt-based fabrication process, ACB pebbles display a characteristic solidification microstructure. Whereas pebbles with a composition near the eutectic exhibit a typical eutectic microstructure with parallel lamellae of LOS and LMT, every now and then intersected by either primary LOS or primary LMT dendrites, the microstructure of pebbles with LMT contents well beyond the eutectic is dominated by finely dispersed LMT dendrites and small grains of LOS (as can be seen in Fig. 6). While the increase in the mechanical strength is caused by the LMT dendrites, the lack of the solubility between the phases limits the diffusion within the system and thus the grain growth. Nearly
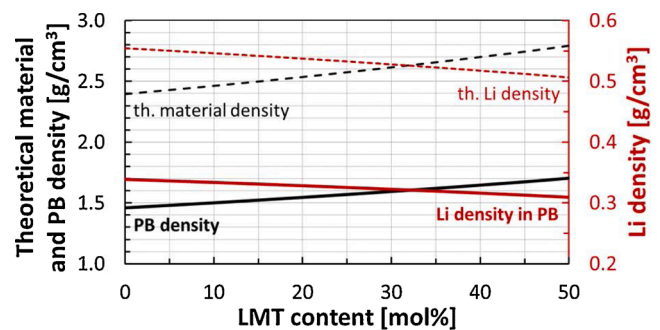

Fig. 2. Theoretical material and Li density, PB density and Li density in PB as a function of the LMT content. (A material density of 95 % and a packing factor of 64.2 % were assumed for the PB.).
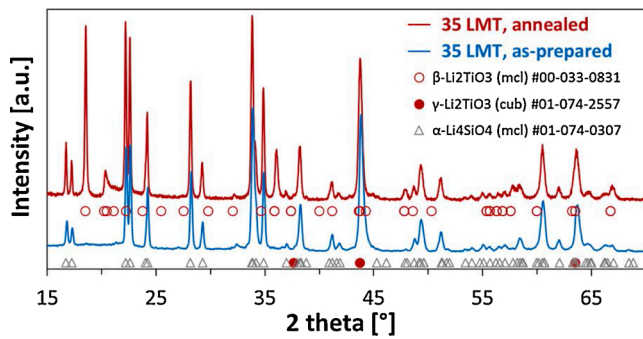
Fig. 3. X-ray diffraction pattern of ACB pebbles with 35 mol% LMT in the as-prepared state (bottom) and after annealing (top).
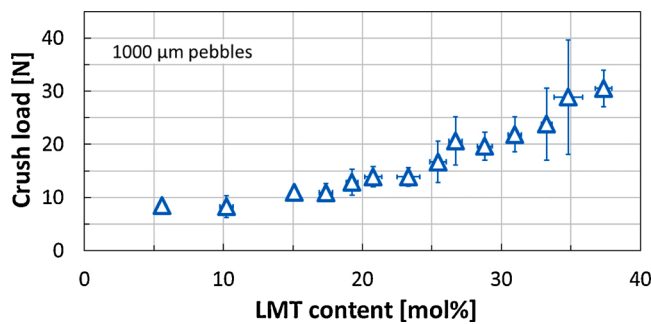

Fig. 4. Average crush load of ACB pebble batches as a function of the LMT content.

independent of the composition, the pebbles exhibit a density of about 95% TD. The porosity of 5 % consists of about equal parts of open and closed porosity. With a packing factor of about 64.2 %, a PB density of 61 % is achieved. Material properties for ACB pebbles with 35 mol% LMT are summarised in Table 1 [4].

3.2. Properties of ACB pebble beds

During operation, breeder PBs will be exposed to harsh operating conditions such as intense neutron radiation, elevated temperatures and thermal cycling. Due to the missing possibility of neutron irradiation experiments, the properties of ACB PBs were assessed in different experiments either to mimic selected conditions or to establish material properties that are important for the design and modelling of the breeder blanket.

The long-term stability of different compositions of ACB pebbles was investigated in long-term annealing experiments at 900 °C under He/0.1 % H_2 as well as He/~0.1 % H_2O purge gas combinations for about 4 months [10]. All investigated compositions showed a high degree of chemical, microstructural and mechanical stability under both purge gas atmospheres. After an initial decrease in the mean crush load during the first day (most likely attributable to the adjustment to the equilibrium

Table 1
Material properties of ACB pebbles with 35 mol% LMT.

Phase composition	65 mol% Li_4SiO_4 + 35 mol% Li_2TiO_3
Theoretical density	2.657 g/cm^3
Rel. pebble density	95 ± 1 %
Pebble density	2.52 ± 0.03 g/cm^3
Total porosity	5 ± 1 %
Open porosity	3 ± 1 %
Closed porosity	2 ± 1 %
Packing factor	64.2 %
Pebble bed density	1.62 ± 0.02 g/cm^3
Melting temperature	~ 1290 °C

phases), the values are maintained at a high level particularly for higher LMT contents and independent of the purge gas composition (exemplarily shown for 35 mol% in Fig. 5). Due to the limited diffusion, the microstructure of the material remains virtually unchanged even after 4 months, with hardly any grain growth of the LMT dendrites and a very limited grain growth of the LOS grains (Fig. 6).

To establish the mechanical and thermomechanical properties of PBs, several intricate experiments were carried out. The mechanical behaviour of PBs, including cyclic loading scenarios, were investigated in several studies along with Discrete Element Method (DEM) simulations [11–13]. It was found that the pebble shape strongly influences the mechanical behaviour of the PB. A softer behaviour of ellipsoidal pebbles and a higher packing factor was found for nonperfect spherical shapes [12]. Subjected to cyclic loading, monosized assemblies showed a stiffer response and a lower residual strain accumulation than polydisperse assemblies. The average normal contact force that the CB pebbles experience is quite low (about 2.5 N), while the majority of the pebbles will experience a maximum normal contact force less than 5 times the average normal force [13]. With measured crush loads well above this value after long-term annealing, a low risk of fragmentation is expected for ACB pebbles during the operation of a HCPB blanket.

For the design of the blanket, the knowledge of the thermal conductivity of the PB is of high importance. An experimental setup was designed and assembled based on the 'hot wire method' to measure the thermal conductivity of the ACB PB in dependence of temperature, compressive load, gas pressure and gas composition [14]. The results showed a negligible influence of the chemical composition of the solid material (20–30 mol% LMT) on the bed's effective thermal conductivity. An increase in the effective thermal conductivity with the temperature was detected in both He and air, while the influence of the compressive load was found to be small. Compared to helium though, air resulted in a severe reduction of the effective thermal conductivity. A clear dependence of the effective thermal conductivity on the pressure of the filling gas was observed in He (Fig. 7) in contrast to air, where the pressure dependence was drastically reduced. The experimental results were successfully used to calibrate a newly developed thermal DEM code [15]. It is now possible to model the effective thermal conductivity of PBs including the dependence on the gas pressure, as well as taking the Smoluchowski effect into account [16]. Additionally, it is possible to evaluate the temperature profile generated by the neutronic heating.

As the knowledge of the thermal diffusivity of the breeder beds is also required to model the transient heat transfer during the power pulses of the fusion machine, the thermal diffusivity of compressed ceramic PBs was measured at temperatures of up to 700 °C under a uniaxial compressive load of 3 MPa [17]. The thermal diffusivity is reduced with increasing temperature. The filling gas pressure, on the other hand, was found to scarcely affect the thermal diffusivity and thus the specific heat capacity of the beds. Significant changes of the specific heat capacity, associated to the phase transitions of LOS, occur in the temperature range 600–740 °C. These phase transitions lie in the projected
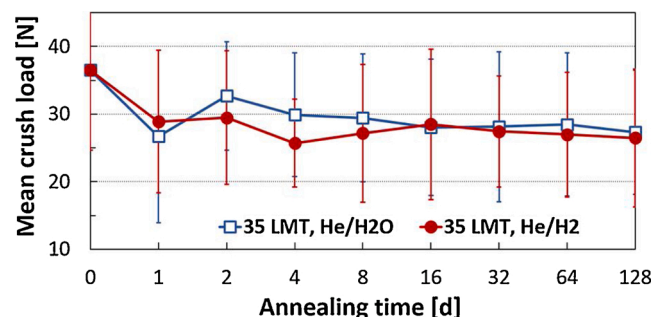

Fig. 5. Development of the mean crush load of ACB pebbles (Ø 1000 μm) with 35 mol% LMT after annealing in dry and humid purge gases at 900 °C after [10].
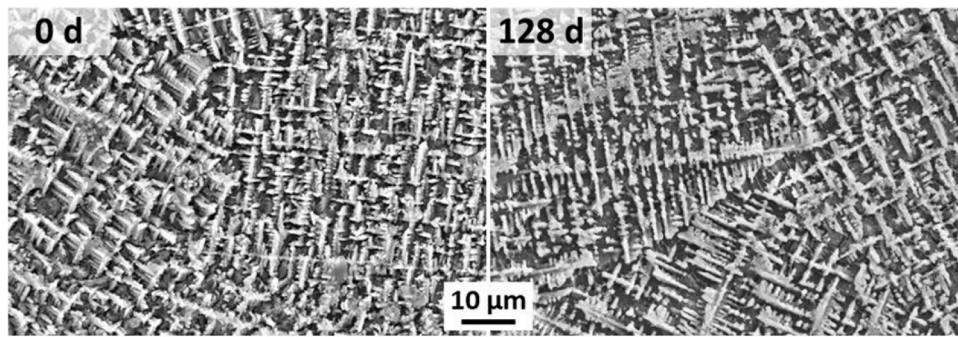
Fig. 6. Microstructure at cross-sections of 35 mol% LMT pebbles in the initial state and after annealing for 128 days under a humid purge gas, after [10].
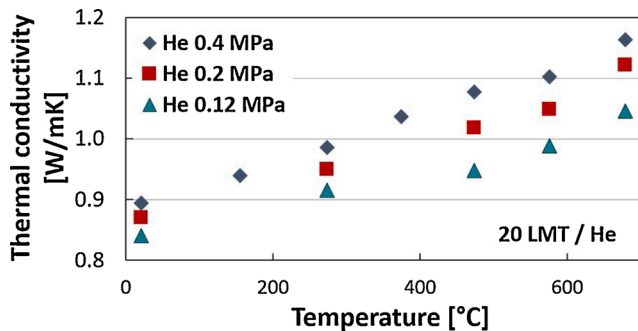

Fig. 7. Gas pressure dependence of the effective thermal conductivity of ACB PBs with 20 mol% LMT in He, after [14].

temperature range that the HCPBs are going to experience during operation in a fusion blanket. It is therefore important that these changes in the specific heat capacity are taken into account for the thermal design of the breeder zone of a solid breeder blanket.

The compatibility between EUROFER and the ACB material was studied in annealing experiments under He/0.1 % H_2 as well as He/~0.1 % H_2O purge gas combinations at different temperatures in collaboration with CIEMAT, Madrid [18–20]. The changes in the ceramics were not significant. Li_2SiO_3 was only generated due to a loss of Li in the surface layer under a humid purge gas at 800 °C; a temperature that is not expected in the contact area between EUROFER and ACB pebbles in the HCPB. In the case of EUROFER, the formation of a double oxide layer was observed. While the attack under a dry purge gas seems to be tolerable, the growth of the corrosion layer was critically enhanced under a humid purge gas, especially at elevated temperatures. While the corrosion layers were rated as tolerable from the chemical point of view, the significant reduction in the fatigue lifetime that was recently observed on EUROFER after contact with the ACB material in preliminary compatibility investigations will have to be pursued further [21]. Additional experiments focusing on the corrosion behaviour of EUROFER with possible coatings were also carried out by CIEMAT [22]. In the presence of LOS, the use of aluminium oxide as a protective coating of EUROFER for the HCPB concept does not seem to be favourable.

Because of the so far lacking possibility for neutron irradiation experiments, several alternative irradiation sources were used. The behaviour of the ACB material and its loading/release characteristics for deuterium were studied under gamma- and electron-irradiation [23] and studies are currently being extended by using ion-irradiation at CIEMAT [24]. Parameters such as loading under simultaneous ionising irradiation or the loading/implanting temperature and their effect on the desorption behaviour are currently being studied. In addition, the radiolysis of ACB pebbles under X-ray and electron irradiation was investigated in collaboration with the University of Latvia in Riga [25–28]. These studies focus on the determination and description of

defect types and their thermal recovery. All these experiments can certainly not compensate for the missing neutron irradiation, but nevertheless give insight to some radiation defects in ACB pebbles and may hint at the temperature range of tritium release. For pure silicate CB, it was recently demonstrated that at least the results obtained for radiation-induced defects and radiolysis products suggest a good comparability of neutron and accelerated electron irradiation. Therefore, effects resulting from ionisation and radiolysis in the material can be well described by irradiation with accelerated electrons [29].

In parallel to the experimental remelting and reprocessing studies [9], the activation behaviour of the ACB material was calculated for multiple usage and melt-based reprocessing cycles under DEMO relevant conditions [30]. After an assumed irradiation of 3 full power years in the reactor, a relatively short waiting time of 18 years was calculated to reach the recycling limit for reprocessing (10^{-2} Sv/h). For the simulated reprocessing loops, it was presumed that the material is stored until the recycling limit is reached and a remelting with re-enrichment can take place. In this scenario, it was calculated that the waiting time for recycling even after the 15th cycle (corresponding to 45 full power years) is only increased to 22 years (Fig. 8).

The increase in the waiting time for recycling is mainly caused by the slight increase in noble metal impurities resulting from the multiple remelting cycles in the Pt alloy crucible. This means that ACB pebbles can be reprocessed (including a Li-6 recycling) using the melt-based process and can be used for many times without the need for a complex and expensive wet-chemical recycling. The waiting time to reach the hands-on level (10^{-5} Sv/h) is prolonged from about 190 years after the 1st cycle to about 625 years after the 15th cycle, mainly because of the long-lived Al-26 isotope as a transmutation product of Si as well as Al impurities [30].

Presently, preparatory activities are ongoing to have a dedicated neutron irradiation experiment for functional materials at ITER relevant conditions (damage dose of 3 dpa in steel) jointly with QST, Japan, under BA DEMO II. With regard to ACB pebbles, it is essential to foremost investigate the in-situ tritium release and tritium residence time, if possible under different purge gas atmospheres. Additionally, the
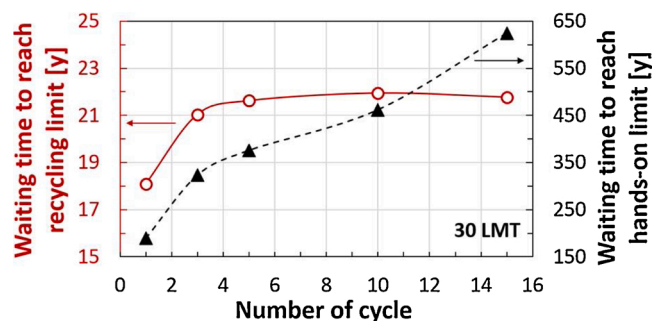

Fig. 8. Calculated waiting time to reach the recycling limit and the hands-on limit for 30 mol% LMT, after [30].

compatibility with EUROFER under irradiation as well as pre-compacted PBs are planned to be investigated. Extensive post irradiation examinations, planned at KIT, will give insight into the development of the microstructure, the porosity and the mechanical properties as well as the phase content. With these results, the material composition of ACB pebbles will also be conclusively determined.

4. Summary

A melt-based fabrication process for the production of ACB pebbles with a high production yield was developed. With the already projected scale-up of KALOS, the process will be transferred to a medium sized production capacity and will be able to cover any needs for breeder blanket mock-ups and ITER TBMs. This larger facility will in principle also demonstrate the transferability to an industrial scale production.

Concerning the material development, the addition of LMT to LOS in ACB pebbles results in a significant increase in the mechanical strength compared to the formerly pursued pure silicate material. The behaviour and characteristics of ACB pebbles and PBs were extensively investigated in several dedicated experiments during the pre-conceptual phase. The ACB pebbles exhibit a superior chemical and thermal stability, and important thermomechanical properties of PBs have been established. Details of the material and PB properties were recently summarised in a Material Property Handbook on ACB [4]. Irradiation experiments using alternatives to neutrons indicate a good radiation stability; however, it is extremely important to investigate the tritium release characteristics of ACB as well as the development of the microstructure under neutron irradiation in the next step.

Declaration of Competing Interest

The authors declare that they have no known competing financial interests or personal relationships that could have appeared to influence the work reported in this paper.

Acknowledgments

References

[1] R. Knitter, P. Chaudhuri, Y.J. Feng, T. Hoshino, I.-K. Yu, Recent developments of solid breeder fabrication, J. Nucl. Mater. 442 (2013) S420–S424, https://doi.org/10.1016/j.jnucmat.2013.02.060.

[2] R. Knitter, M.H.H. Kolb, U. Kaufmann, A.A. Goraieb, Fabrication of modified lithium orthosilicate pebbles by addition of titania, J. Nucl. Mater. 442 (2013) S433–S436, https://doi.org/10.1016/j.jnucmat.2012.10.034.

[3] M.H.H. Kolb, R. Knitter, U. Kaufmann, D. Mundt, Enhanced fabrication process for lithium orthosilicate pebbles as breeding material, Fusion Eng. Des. 86 (2011) 2148–2151, https://doi.org/10.1016/j.fusengdes.2011.01.104.

[4] J.M. Heuser, O. Leys, R. Knitter, Material Property Handbook on Advanced Ceramic Breeder, BB-1.3.1-T007-D008, 2019, https://idm.euro-fusion.org/?uid=2NVAS9.

[5] P. Waibel, J. Matthes, O. Leys, M. Kolb, H.B. Keller, R. Knitter, High-speed camera-based analysis of the lithium ceramic pebble fabrication process, Chem. Eng. Technol. 37 (2014) 1654–1662, https://doi.org/10.1002/ceat.201300769.

[6] O. Leys, P. Waibel, J. Matthes, H. Keller, R. Knitter, Characterisation of high-temperature jet break-up for ceramic sphere production, Int. J. Adv. Manuf. Technol. 98 (2018) 2311–2318, https://doi.org/10.1007/s00170-018-2378-y.

[7] O. Leys, P. Waibel, J. Matthes, R. Knitter, Ceramic pebble production from the break-up of a molten laminar jet, Proceedings of ILASS–Europe 2019, 29th European Conference on Liquid Atomization and Spray Systems (2019). https://ilass19.sciencesconf.org/244756.

[8] R. Knitter, B. Löbbecke, Reprocessing of lithium orthosilicate breeder material by remelting, J. Nucl. Mater. 361 (2007) 104–111, https://doi.org/10.1016/j.jnucmat.2006.11.005.

[9] O. Leys, T. Bergfeldt, M.H.H. Kolb, R. Knitter, The reprocessing of advanced mixed lithium orthosilicate/metatitanate tritium breeder pebbles, Fusion Eng. Des. 107 (2016) 70–74, https://doi.org/10.1016/j.fusengdes.2016.04.025.

[10] J.M. Heuser, M.H.H. Kolb, T. Bergfeldt, R. Knitter, Long-term thermal stability of two-phased lithium orthosilicate/metatitanate ceramics, J. Nucl. Mater. 507 (2018) 396–402, https://doi.org/10.1016/j.jnucmat.2018.05.010.

[11] S. Pupeschi, R. Knitter, M. Kamlah, Y. Gan, Numerical and experimental characterization of ceramic pebble beds under cycling mechanical loading, Fusion Eng. Des. 112 (2016) 162–168, https://doi.org/10.1016/j.fusengdes.2016.08.021.

[12] M. Moscardini, Y. Gan, R.K. Annabattula, M. Kamlah, A Discrete element method to simulate the mechanical behavior of ellipsoidal particles for a fusion breeding blanket, Fusion Eng. Des. 121 (2017) 22–31, https://doi.org/10.1016/j.fusengdes.2017.05.110.

[13] S. Pupeschi, M. Moscardini, Y. Gan, R. Knitter, M. Kamlah, Cyclic behavior of ceramic pebble beds under mechanical loading, Fusion Eng. Des. 134 (2018) 11–21, https://doi.org/10.1016/j.fusengdes.2018.06.009.

[14] S. Pupeschi, R. Knitter, M. Kamlah, Effective thermal conductivity of advanced ceramic breeder pebble beds, Fusion Eng. Des. 116 (2017) 73–80, https://doi.org/10.1016/j.fusengdes.2017.01.026.

[15] M. Moscardini, Y. Gan, S. Pupeschi, M. Kamlah, Discrete element method for effective thermal conductivity of packed pebbles accounting for the Smoluchowski effect, Fusion Eng. Des. 127 (2018) 192–201, https://doi.org/10.1016/j.fusengdes.2018.01.013.

[16] M. Moscardini, S. Pupeschi, Y. Gan, F.A. Hernández, M. Kamlah, Discrete element analysis of heat transfer in the breeder beds of the European solid breeder blanket concept, Fusion Sci. Technol. 75 (4) (2019) 283–4298, https://doi.org/10.1080/15361055.2019.1565481.

[17] S. Pupeschi, M.H.H. Kolb, R. Knitter, Experimental investigation of thermal diffusivity and heat capacity of ceramic breeder beds, J. Nucl. Mater. 518 (2019) 400–408, https://doi.org/10.1016/j.jnucmat.2019.03.002.

[18] K. Mukai, F. Sánchez, R. Knitter, Chemical compatibility study between ceramic breeder and EUROFER97 steel for HCPB-DEMO blanket, J. Nucl. Mater. 488 (2017) 196–203, https://doi.org/10.1016/j.jnucmat.2017.03.018.

[19] K. Mukai, M. Gonzalez, R. Knitter, Effect of moisture in sweep gas on chemical compatibility between ceramic breeder and EUROFER97, Fusion Eng. Des. 125 (2017) 154–159, https://doi.org/10.1016/j.fusengdes.2017.10.001.

[20] T. Hernández, M. Carmona Gázquez, F.J. Sánchez, M. Malo, Corrosion mechanisms of Eurofer produced by lithium ceramics under fusion relevant conditions, Nucl. Mater. Energy 15 (2018) 110–114, https://doi.org/10.1016/j.nme.2018.03.005.

[21] J. Aktaa, M. Walter, E. Gaisina, M.H.H. Kolb, R. Knitter, Assessment of the chemical compatibility between EUROFER and ceramic breeder with respect to fatigue lifetime, Fusion Eng. Des. 157 (2020), 111732, https://doi.org/10.1016/j.fusengdes.2020.111732.

[22] T. Hernández, F.J. Sánchez, F. Di Fonzo, M. Vanazzi, M. Panizo, R. González-Arrabal, Corrosion protective action of different coatings for the helium cooled pebble bed breeder concept, J. Nucl. Mater. 516 (2019) 160–168, https://doi.org/10.1016/j.jnucmat.2019.01.009.

[23] M. González, E. Carella, A. Moroño, M.H.H. Kolb, R. Knitter, Thermally induced outdiffusion studies of deuterium in ceramic breeder blanket materials after irradiation, Fusion Eng. Des. 98-99 (2015) 1771–1774, https://doi.org/10.1016/j.fusengdes.2015.03.027.

[24] M. González, M. Malo, F. Sánchez, Behavior of ceramic breeder candidates under high-energy ion beams, Proceedings of CBBI-20 (2019) 128–143, https://doi.org/10.5445/IR/1000100675.

[25] A. Zarins, O. Valtenbergs, G. Kizane, A. Supe, R. Knitter, M.H.H. Kolb, O. Leys, L. Baumane, D. Conka, Formation and accumulation of radiation-induced defects and radiolysis products in modified lithium orthosilicate pebbles with additions of titanium dioxide, J. Nucl. Mater. 470 (2016) 187–196, https://doi.org/10.1016/j.jnucmat.2015.12.027.

[26] A. Zarins, O. Leys, G. Kizane, A. Supe, L. Baumane, M. González, V. Correcher, C. Boronat, A. Zolotarjovs, R. Knitter, Behaviour of advanced tritium breeder pebbles under simultaneous action of accelerated electrons and high temperature, Fusion Eng. Des. 121 (2017) 167–173, https://doi.org/10.1016/j.fusengdes.2017.06.033.

[27] J.M. Heuser, A. Zarins, L. Baumane, G. Kizane, R. Knitter, Radiation stability of long-term annealed bi-phasic advanced ceramic breeder pebbles, Fusion Eng. Des. 138 (2019) 395–399, https://doi.org/10.1016/j.fusengdes.2018.12.034.

[28] J. Cipa, A. Zarins, A. Supe, G. Kizane, A. Zolotarjovs, L. Baumane, L. Trinkler, O. Leys, R. Knitter, X-ray induced defects in advanced lithium orthosilicate pebbles with additions of lithium metatitanate, Fusion Eng. Des. 143 (2019) 10–15, https://doi.org/10.1016/j.fusengdes.2019.03.096.

[29] J.M. Leys, A. Zarins, J. Cipa, L. Baumane, G. Kizane, R. Knitter, Radiation-induced effects in neutron- and electron-irradiated lithium silicate ceramic breeder pebbles, J. Nucl. Mater. 540 (2020) 152347, https://doi.org/10.1016/j.jnucmat.2020.152347.

[30] K. Mukai, P. Pereslavtsev, U. Fischer, R. Knitter, Activation calculations for multiple recycling of breeder ceramics by melt processing, Fusion Eng. Des. 100 (2015) 565–570, https://doi.org/10.1016/j.fusengdes.2015.08.007.